

## 2D-IR Study of a Photoswitchable Isotope-Labeled $\alpha$ -Helix

Ellen H. G. Backus,<sup>†,‡</sup> Robbert Bloem,<sup>‡</sup> Paul M. Donaldson,<sup>‡</sup> Janne A. Ihalainen,<sup>‡,§</sup>  
Rolf Pfister,<sup>‡</sup> Beatrice Paoli,<sup>||</sup> Amedeo Caffisch,<sup>||</sup> and Peter Hamm<sup>\*,‡</sup>

FOM Institute for Atomic and Molecular Physics, Science Park 104, 1098 XG Amsterdam, The Netherlands, Physikalisch-Chemisches Institut, Universität Zürich, Winterthurerstrasse 190, CH-8057 Zürich, Switzerland, Nanoscience Centre, Department of Biological and Environmental Science, University of Jyväskylä, P.O. Box 35, FIN-40014 Jyväskylä, Finland, and Biochemisches Institut, Universität Zürich, Winterthurerstrasse 190, CH-8057 Zürich, Switzerland

Received: December 15, 2009; Revised Manuscript Received: January 27, 2010

A series of photoswitchable,  $\alpha$ -helical peptides were studied using two-dimensional infrared spectroscopy (2D-IR). Single-isotope labeling with  $^{13}\text{C}^{18}\text{O}$  at various positions in the sequence was employed to spectrally isolate particular backbone positions. We show that a single  $^{13}\text{C}^{18}\text{O}$  label can give rise to two bands along the diagonal of the 2D-IR spectrum, one of which is from an amide group that is hydrogen-bonded internally, or to a solvent molecule, and the other from a non-hydrogen-bonded amide group. The photoswitch enabled examination of both the folded and unfolded state of the helix. For most sites, unfolding of the peptide caused a shift of intensity from the hydrogen-bonded peak to the non-hydrogen-bonded peak. The relative intensity of the two diagonal peaks gives an indication of the fraction of molecules hydrogen-bonded at a certain location along the sequence. As this fraction varies quite substantially along the helix, we conclude that the helix is not uniformly folded. Furthermore, the shift in hydrogen bonding is much smaller than the change of helicity measured by CD spectroscopy, indicating that non-native hydrogen-bonded or mis-folded loops are formed in the unfolded ensemble.

### Introduction

Two-dimensional infrared spectroscopy has the potential to unravel information about molecular structure and dynamics which cannot be obtained from a linear spectrum. Although the diagonal peaks resemble in principle the linear absorption spectrum, two absorption bands close in frequency are better resolved on the diagonal in the 2D-IR spectrum than in the linear spectrum, because the intensity scales quadratically with extinction coefficient in a 2D-IR spectrum; i.e., backgrounds from weak but higher concentration bands, such as from the solvent, are very efficiently suppressed.<sup>1</sup> Moreover, the line shape of the diagonal peaks show clearly the contributions of homogeneous and inhomogeneous broadening.<sup>2</sup> The separation between the bleach and excited state absorption reports on the system's anharmonicity. In addition to the diagonal peaks, a 2D-IR spectrum might have off-diagonal features (cross-peaks). For instance, if two molecular groups are close to each other in space, the two vibrational transitions might couple, resulting in a cross-peak in the 2D-IR spectrum, giving structural information.<sup>3–8</sup> An off-diagonal peak could also occur if two diagonal peaks originate from two different species which exchange on the time scale of the experiment.<sup>9–11</sup>

As 2D-IR spectroscopy becomes a more developed technique, the complexity of the systems studied with it is increasing. In the early stages, for the biophysical field, a lot of work was carried out on simple model systems like *N*-methyl acetamide (NMA)<sup>9</sup> and small peptides<sup>3,12,13</sup> focusing on the amide I vibration. More recently, large peptides<sup>14,15</sup> and proteins<sup>5,16</sup> sometimes even embedded in a membrane<sup>17,18</sup> have been studied.

To obtain site selective information, 2D-IR spectroscopy is often used in combination with isotope labeling<sup>14,17,18</sup> to spectrally isolate one vibration from all of the others.

Hochstrasser and co-workers have studied the 2D-IR spectroscopy of  $\alpha$ -helical peptides, employing extensive isotope labeling.<sup>14,19</sup> Nevertheless, we are not aware of any systematic study of 2D-IR spectroscopy in relation to the degree of helicity of a peptide. It is well-known that the amide I vibration shifts to a lower frequency by about 20  $\text{cm}^{-1}$  upon hydrogen bonding.<sup>20</sup> This effect has been shown clearly for a solution of NMA, the prototype molecule for the amide I vibration, in methanol. In this case, a close to 50%/50% equilibrium exists between single and double hydrogen-bonded forms of the NMA-carbonyl group,<sup>21</sup> giving rise to a double peak structure that has been investigated with linear absorption and 2D-IR spectroscopy.<sup>9</sup> Intramolecular hydrogen bonding is the major reason for the overall frequency shift of the amide I band upon helix formation, and has been used before in numerous studies utilizing linear absorption spectroscopy.<sup>22–24</sup> Here, we will expand this type of study to 2D-IR spectroscopy. One way of decreasing the helicity of a peptide would be by increasing the temperature.<sup>25–29</sup> However, vibrational transitions would also broaden as a result of the elevated temperature, complicating the interpretation of the spectra.

As another way to control the helicity, we utilize here a photoswitch attached to a peptide in such a way that it stabilizes or destabilizes its helical content depending on the conformation of the photoswitch. We use an azobenzene moiety which has been used recently in a number of studies<sup>24,30–35</sup> as a photoswitch (Figure 1). If the azobenzene switch is in the *trans* state, its end-to-end distance roughly matches three helix loops, thereby stabilizing the helicity of the peptide. In contrast, in the *cis* state, the end-to-end distance is too small and the helix is severely

<sup>†</sup> FOM Institute for Atomic and Molecular Physics.

<sup>‡</sup> Physikalisch-Chemisches Institut, Universität Zürich.

<sup>§</sup> University of Jyväskylä.

<sup>||</sup> Biochemisches Institut, Universität Zürich.

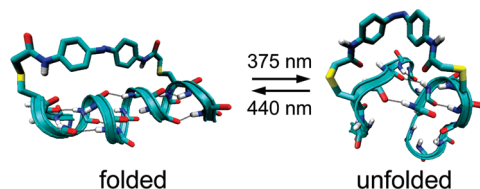


**Figure 1.** Schematic drawing of the peptide with the azobenzene moiety in the folded (azobenzene in *trans* conformation) and unfolded (*cis* conformation of azobenzene) state.<sup>52</sup>

destabilized. The amino acid sequence for the peptides explored here has high helix propensity, Ac-AACAK<sup>5</sup>AAAAK<sup>10</sup>AAACK<sup>15</sup>A-NH<sub>2</sub>. The azobenzene moiety is attached via the two cysteines. Switching the azobenzene switch from the *trans* to the *cis* state reduced the helicity of the peptide from roughly 70 to 20% at  $T = 4$  °C, as judged from CD spectroscopy.<sup>24</sup> To obtain site specific information, isotope labeled amino acids were incorporated. We used <sup>13</sup>C<sup>18</sup>O labeled amino acids, which lowers the vibrational frequency of the amide I vibration by  $\sim 70$  cm<sup>-1</sup>.<sup>14,19,36</sup> As we will see, the frequency shift of <sup>13</sup>C<sup>16</sup>O ( $\sim 35$  cm<sup>-1</sup>) is not necessarily sufficient to truly separate the band from the main amide I band.<sup>37,38</sup>

Four different isotopomers were investigated—L4, L7, L9, and L11—where the number identifies the <sup>13</sup>C<sup>18</sup>O labeled site counted from the N-terminus. For comparison, we will also present data on double-labeled samples, i.e., one amino acid <sup>13</sup>C<sup>18</sup>O labeled and another <sup>13</sup>C<sup>16</sup>O labeled. Specifically, we will present 2D-IR spectra of L47, L74, and L96, where the first and second number specifies the <sup>13</sup>C<sup>18</sup>O and <sup>13</sup>C<sup>16</sup>O labeled amino acid, respectively. Our experimental data are corroborated by simulated 2D spectra based on molecular structures obtained by MD simulations.

## Experimental Section

Infrared absorption spectra were collected on a commercial Fourier transform infrared spectrometer (FTS 175 C, Bio-Rad). 2D-IR spectra were measured with a revised version of the home-built actively phase-stabilized 2D-IR photon echo setup described previously.<sup>39,40</sup> Briefly, an IR pulse (1580 cm<sup>-1</sup>,  $\sim 100$  fs and 140 cm<sup>-1</sup> fwhm) generated by a Ti:S pumped OPA combined with a difference frequency mixing stage was split into three equally strong pulses ( $\sim 0.5$   $\mu$ J each) to excite the sample and into two weak pulses (a local oscillator, LO, and a tracer beam for alignment purposes). To avoid unbalanced chirps in the pulses, compensation plates were used to make the amount of glass the same in the pulse pairs. The third order polarization emitted in the  $-k_1 + k_2 + k_3$  direction was interfered with the LO in a balanced detection arrangement<sup>41,42</sup> and the two outputs subsequently dispersed in a spectrometer (Triax Series) and each imaged onto 31 pixels of an array detector (Infrared Associates). The two signals from the balanced detection were subtracted to retrieve the third order signal. Pulse  $k_3$  was phase cycled by means of a photoelastic modulator to remove scattering.<sup>43</sup> Purely absorptive 2D-IR spectra were obtained by summing the rephasing and nonrephasing signals, which were obtained by interchanging the time ordering of pulses 1 and 2. All beams were polarized in parallel.

The data were collected with time steps of 25.34 fs (locked to the HeNe wavelength,<sup>40</sup> under-sampling, vibrational period of amide I' is  $\sim 20$  fs) up to 6.5 ps for both the rephasing and nonrephasing signals, resulting in a spectral resolution after Fourier transformation of  $\sim 5$  cm<sup>-1</sup> along the pump axis. The spectral resolution of the spectrometer (probe axis) was 3.75

and 2.4 cm<sup>-1</sup> for the single and double isotope labeled data, respectively. The waiting time  $T$  was set to 300 fs.

Phasing of the 2D-IR spectra was performed by comparing the projection of the purely absorptive 2D spectrum onto the probe frequency axis to a pump–probe spectrum recorded after broadband excitation (projection slice theorem).<sup>44</sup> Since the pump–probe signal for the isotope label is very small, we used either the main band at  $\sim 1640$  cm<sup>-1</sup> or the signal from NMA dissolved in water for determining the phase (the spectral phase is basically constant over the IR pulse). The correctness of this procedure was double-checked by comparing the photon-echo 2D spectra after rephasing with pump–probe 2D data for some of the samples.

The  $\alpha$ -helical peptide (sequence Ac-<sup>1</sup>AACAK<sup>5</sup>AAAAK<sup>10</sup>-AAACK<sup>15</sup>A-NH<sub>2</sub>) was prepared by standard Fmoc-based solid phase peptide synthesis methods (GL Biochem Ltd. Shanghai). The <sup>18</sup>O amino acid was prepared by H<sub>2</sub><sup>18</sup>O exchange.<sup>45</sup> The natural abundance of <sup>13</sup>C results in roughly 16% of the helices having a randomly distributed <sup>13</sup>C<sup>16</sup>O group present in the peptide. In addition, the <sup>13</sup>C<sup>16</sup>O group brought in on purpose is present for the double-labeled peptides (L47, L74, and L96). From mass spectrometry, we conclude that in the double labeled peptides at least 85% of the molecules have both <sup>13</sup>C<sup>18</sup>O and <sup>13</sup>C<sup>16</sup>O labels, while in the single labeled peptides more than 99% has a <sup>13</sup>C<sup>18</sup>O label.

The photoswitch was linked to the cysteines as described earlier.<sup>30</sup> To minimize perturbation of the amide I' region of the spectrum by vibrational transitions from the photoswitch, the benzene rings were completely <sup>13</sup>C labeled.<sup>46</sup> After removing TFA by liquid chromatography, the samples were dissolved in 10 mM phosphate buffer (D<sub>2</sub>O, pD  $\sim 6$ ) at a concentration of  $\sim 3$  mM. This was just below the onset of aggregation (at higher concentrations, FTIR difference spectra became concentration dependent). The samples were held between two CaF<sub>2</sub> windows with a 30  $\mu$ m spacer for both the linear absorption and the 2D-IR measurements. The *cis* state of the photoswitch was prepared by irradiating the samples with a light emitting diode (LED) at 375 nm ( $\sim 15$  mW, fwhm 12 nm). The thermodynamically more stable *trans* state could be reobtained by raising the sample's temperature to 40 °C for a few minutes. The experiments were performed at 4 °C, to maximize the change of helicity between both states, and to obtain as narrow as possible absorption lines.

Simulations of 2D-IR spectra are based on equilibrium MD simulations of a similar cross-linked peptide (i.e., Ac-AACAR<sup>5</sup>AAAAAR<sup>10</sup>AAACR<sup>15</sup>A-NH<sub>2</sub>) with the azo-linker in either the *cis* or the *trans* configuration. In total, 1000 statistically independent snapshot structures, spaced by 10 ns, at 281 K were obtained for each conformation from a 10  $\mu$ s replica-exchange molecular dynamics simulation (REMD) with implicit solvent (see ref 24 for simulation details).

For each snapshot structure, we calculated a spectroscopic Hamiltonian for the amide I modes along the lines of ref 47. Nearest neighbor coupling between amide I vibrations was taken from a ( $\phi, \psi$ )-dihedral map which has been precalculated on the B3LYP 6-31+G\* level of theory.<sup>48</sup> The coupling of more distant peptide units was calculated according to the transition charge model. The intrinsic (uncoupled, unlabeled, and non-hydrogen-bonded) amide I frequencies of all sites were fixed to 1655 cm<sup>-1</sup>. <sup>13</sup>C<sup>18</sup>O isotope labeling was introduced by lowering the corresponding amide I frequency by  $-69$  cm<sup>-1</sup>.<sup>49</sup> The additional effect of hydrogen bonding to either the backbone, the azo-linker, or the guanidinium group of the Arg side chains was taken into account by introducing an additional frequency shift:

$$\delta\omega = -\Delta(2.6 \text{ \AA} - r_{\text{O}\dots\text{H}})$$

whenever the hydrogen-bond length  $r_{\text{O}\dots\text{H}}$  was shorter than the threshold value of 2.6 Å. We considered only hydrogen bonds with an angle smaller than 60° but found that this threshold does not make any qualitative difference. The proportionality constant was set to  $\Delta = 30 \text{ cm}^{-1}/\text{Å}$ , resulting in a hydrogen bond shift of ca. 20  $\text{cm}^{-1}$  at a typical hydrogen bond distance of 2 Å. As the MD simulation was with implicit water to allow for a full sampling of the conformation space, we could not introduce the effect of hydrogen bonding to water molecules. The C=O local mode anharmonicity was set to 16  $\text{cm}^{-1}$ . The spectroscopic Hamiltonian was diagonalized, each transition was masked with a homogeneous width of 10  $\text{cm}^{-1}$  (fwhm), and the resulting 2D-IR spectra were averaged over the 1000 snapshot structures from the REMD simulation.

## Results

In Figure 2, the IR absorption spectra for four different peptides in the folded state (*trans* configuration of the photo-switch), with a  $^{13}\text{C}^{18}\text{O}$  isotope label at position 4, 7, 9, or 11 along the helix, are plotted in black. For all peptides, we observe a strong absorption band at  $\sim 1640 \text{ cm}^{-1}$ , originating from the amide I' mode (C=O stretch vibration) of all nonisotope labeled amino acids. The small peak at  $1545 \text{ cm}^{-1}$ , visible for all peptides, is assigned to ring modes of the  $^{13}\text{C}$  labeled azobenzene moiety.<sup>46</sup> Furthermore, the spectra show small absorption bands at  $\sim 1570$  and/or  $1590 \text{ cm}^{-1}$ , which will be assigned below. Upon irradiation with the LED initiating unfolding of the peptide, the spectrum slightly changes (Figure 2, red lines). The main band shifts to higher frequency and the intensity of the small bands at  $1570$  and  $1590 \text{ cm}^{-1}$  also changes. The spectral changes between the folded and unfolded spectra are clearer in the difference spectra (folded minus unfolded state, gray curves in Figure 2).

The 2D-IR spectra of the four single-isotope labeled samples in the folded state (*trans* configuration of the photo-switch) are depicted in the left column of Figure 3 where we focused on the region between  $1525$  and  $1640 \text{ cm}^{-1}$ . All spectra show peaks on the diagonal, which to a great extent parallel the absorption spectra presented in Figure 2. However, the appearance of the peaks is much more pronounced in the 2D-IR spectra, because background bands are suppressed due to the nonlinear nature of the 2D-IR response.<sup>1</sup> Moreover, the anharmonicity of the main band is smaller due to its delocalization, enhancing the 2D-IR bands of the isotope labeled group in a relative sense.

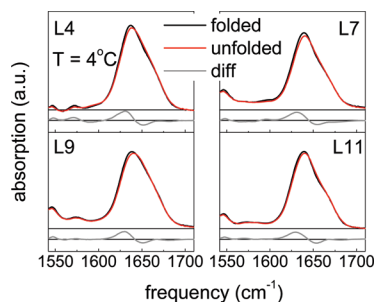


**Figure 2.** Infrared absorption spectra of four different peptides of 16 amino acids with one amino acid along the chain labeled with  $^{13}\text{C}^{18}\text{O}$  for the folded and the unfolded state. At the bottom of every panel, the difference spectrum (offset and multiplied by 2) is depicted as folded minus unfolded state. Isotopomers L4, L7, L9, and L11 have been measured, where the number refers to the position of a  $^{13}\text{C}^{18}\text{O}$  labeled amino acid in the sequence. All spectra were measured at  $T = 4 \text{ }^\circ\text{C}$ .

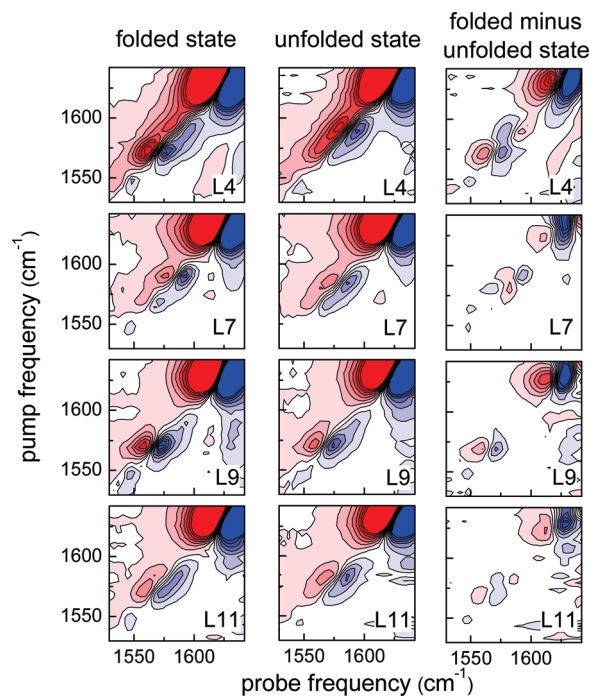


**Figure 3.** Purely absorptive 2D-IR spectra of the peptides in the folded (left) and unfolded (middle) state taken at  $T = 4 \text{ }^\circ\text{C}$ . The right panel shows the spectra for the folded minus the unfolded state. Blue and red colors indicate negative and positive absorption change, respectively. The contour lines represent a linear scale. All spectra are plotted with the same intensity scaling.

Clearly, L4 has two peaks, one at  $1570 \text{ cm}^{-1}$  and a weaker one at  $1590 \text{ cm}^{-1}$ . In contrast, L7 has a strong peak around  $1590$  and a weak one at the other position. L9 shows the peak at the lowest frequency with a small shoulder at high frequency, while L11 has both peaks with roughly equal intensity. In none of the spectra, a cross-peak between the two peaks at  $1570$  and  $1590 \text{ cm}^{-1}$  is observed. Some spectra show cross-peaks between these two bands and the main band (lower right corner), which reflect the coupling of the labeled unit to the rest of the helix.

One might argue that the naturally present  $^{13}\text{C}^{16}\text{O}$  (in  $\sim 16\%$  of the helices) gives rise to the band at  $1590 \text{ cm}^{-1}$ . However, on the basis of the reduced mass, this vibrational transition is expected at  $1605 \text{ cm}^{-1}$ . Moreover, if the band originates from  $^{13}\text{C}^{16}\text{O}$ , one would expect the intensity of the band to increase in double labeled samples where essentially all peptides have a  $^{13}\text{C}^{16}\text{O}$  label instead of the naturally abundant 16%. Figures 4 and 5 depict linear absorption and 2D-IR spectra of the double labeled samples L47 (i.e.,  $^{13}\text{C}^{18}\text{O}$  at position 4,  $^{13}\text{C}^{16}\text{O}$  at position 7), L74, and L96. Clearly, for L47 and L74, the expected increase in the band at  $1590 \text{ cm}^{-1}$  is not visible; the spectra of L47 and L74 look essentially the same as those of L4 and L7, respectively. For L96, in contrast, a peak at  $1590 \text{ cm}^{-1}$  appears that is hardly present in L9, which indeed seems to originate from  $^{13}\text{C}^{16}\text{O}$ . Apparently,  $^{13}\text{C}^{16}\text{O}$  labeling is not always sufficient to safely isolate the amide I' vibration from the main band. Surprisingly, at least for L47 and L74, the two bands at  $1570$  and  $1590 \text{ cm}^{-1}$  originate from one and the same  $^{13}\text{C}^{18}\text{O}$  isotope label, and must reflect a structurally inhomogeneous sample.

To learn about the origin of the two  $^{13}\text{C}^{18}\text{O}$  bands, we investigate in the following how they change upon unfolding of the molecule (achieved by irradiating the sample with an LED at 375 nm). Again, the 2D-IR spectrum consists mainly of diagonal peaks (Figure 3, middle panel). By comparing the left and middle panels of Figure 3, we observe mainly intensity

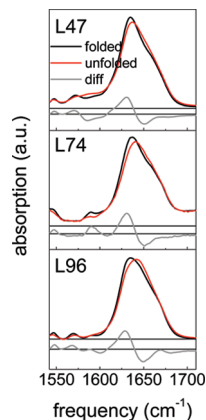


**Figure 4.** Infrared absorption spectra of the double labeled peptides in both the folded and unfolded state. One amino acid along the chain has been labeled with  $^{13}\text{C}^{18}\text{O}$  and a second one with  $^{13}\text{C}^{16}\text{O}$ . At the bottom of every panel, the difference spectrum (offset and multiplied by 2) is depicted as folded minus unfolded conformation. Isotopomers L47, L74, and L96 have been measured, where the first and second number refers to the position of a  $^{13}\text{C}^{18}\text{O}$  and a  $^{13}\text{C}^{16}\text{O}$  labeled amino acid, respectively. The spectra were measured at  $T = 4^\circ\text{C}$ .

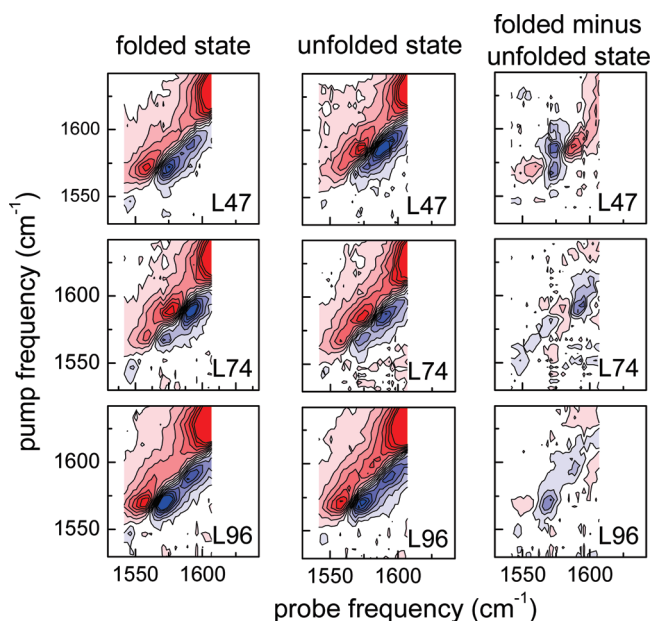


**Figure 5.** Purely absorptive 2D-IR spectra of the double labeled peptides in the folded (left) and unfolded (middle) state taken at  $T = 4^\circ\text{C}$ . The right panel shows the spectra for the folded minus the unfolded state. Blue and red colors indicate negative and positive absorption change, respectively. The contour lines represent a linear scale. All spectra are plotted with the same intensity scaling.

shifts between the two peaks, which are most obvious for L4, where the high frequency absorption band is now the most intense one in the unfolded state. For L7, the lower frequency band gets relatively more intense and the higher frequency band shifts to lower frequency. In contrast, for L9, not much difference between the folded and unfolded state is observed besides a small intensity decrease. The high frequency peak for L11 gains some intensity upon unfolding. The double labeled samples L47 and L74 show exactly the same behavior as L4 and L7, respectively, upon unfolding (Figure 5). Moreover, in general, the peaks of the unfolded state look slightly more tilted along the diagonal than the ones for the folded state, illustrating that the unfolded state is structurally more inhomogeneous.<sup>24,32,50</sup>

To stress the influence of the helicity on the 2D-IR spectrum, we plot in the right panel of Figures 3 and 5 the difference

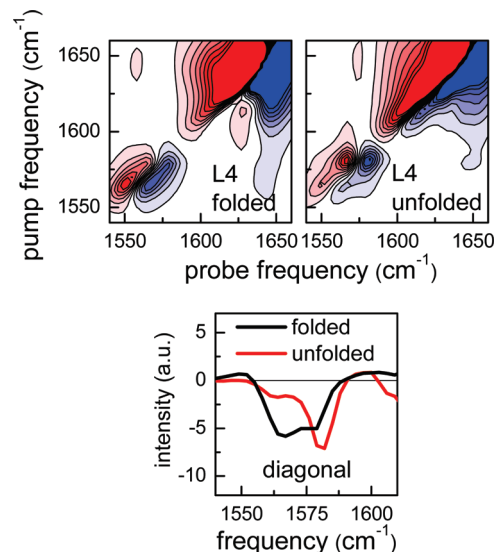


**Figure 6.** Top: Simulated purely absorptive 2D spectra for the single labeled peptide L4 at  $T = 8^\circ\text{C}$  in the folded (left) and unfolded (right) state. The number refers to the position of a  $^{13}\text{C}^{18}\text{O}$  labeled amino acid in the sequence. Bottom: diagonal cut through the 2D spectra. Note the different scaling of the  $x$ -axis in the bottom panel.

between the molecule in the folded and unfolded state (high helicity minus low helicity). Again, all major changes are on the diagonal. A plus/minus feature in the difference spectrum of L9, encoded by the colors blue/red, indicates a decrease of band intensity.<sup>51</sup> The blue-red/red-blue pattern for L4 and L11 represents population transfer from the low frequency band to the high frequency one (i.e., decrease of intensity of the low-frequency band and increase of intensity of the high-frequency band). Due to the proximity of the two bands, the two blue features merge into one. L7 shows the opposite of L4, indicating population transfer from the high frequency peak to the low frequency one upon unfolding.

## Discussion

Two bands for one  $^{13}\text{C}^{18}\text{O}$  isotope label must indicate that there are two distinctively different conformations for each carbonyl group. From DFT calculations, it is known that a hydrogen bond lowers the vibrational frequency of an amide I band by roughly  $20\text{ cm}^{-1}$ .<sup>20</sup> Also, for a small peptide in acetonitrile, two peaks with a difference of  $\sim 20\text{ cm}^{-1}$  have been observed for a particular amide I mode. These were assigned to a closed ring with an intramolecular hydrogen bond and an open structure without a hydrogen bond.<sup>7</sup> In line with this previous work, we assign the double-peak structure observed in our data as from an essentially free  $\text{C}=\text{O}$  group and from a hydrogen-bonded  $\text{C}=\text{O}$  group. The hydrogen bond (to the backbone, to a lysine side-chain, or potentially to a surrounding water molecule) is responsible for the  $\sim 20\text{ cm}^{-1}$  downshifted band. Since the two bands come from different molecules, this also explains why no cross-peaks due to direct couplings are observed.<sup>3-8</sup> Furthermore, on the time scale of this experiment, we do not expect any exchange process to happen,<sup>9-11</sup> since the kinetics of hydrogen bonding is dictated by the relatively slow backbone dynamics.

This peak assignment is corroborated by spectral simulations. For one particular sample, L4, the 2D spectra in the folded and unfolded state together with the diagonal cuts are depicted in Figure 6. Clearly, the spectrum shows the two bands at around  $1570$  and  $1590\text{ cm}^{-1}$  like the experimental spectra in Figure 3.

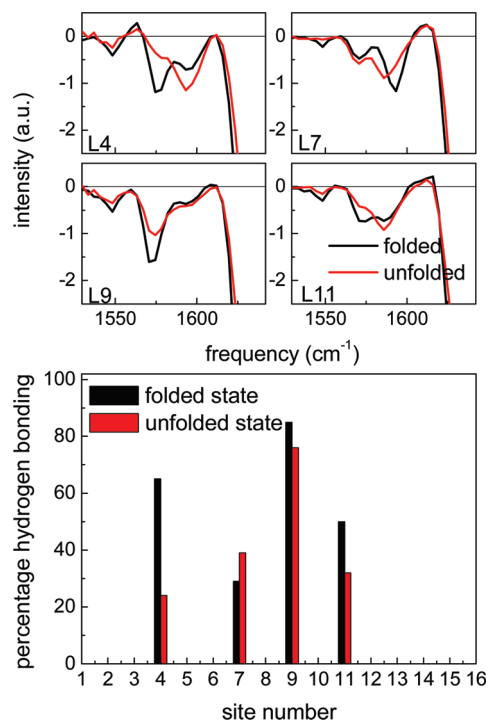


**Figure 7.** Top: Diagonal cuts through the 2D-IR spectra of the folded and unfolded state of Figure 3. To obtain these diagonal cuts, the data are zero padded so that the resolution on the pump axis matches the one on the probe axis. Bottom: Relative amount of hydrogen-bonded species (peak height of low frequency peak divided by the sum of the peak heights of the low and high frequency peak).

Moreover, upon unfolding the peptide, the high frequency peak gains intensity, while the low frequency peak loses intensity. The important outcome of this simulation is, like in the experimental spectra, the bimodal hydrogen-bond distribution, i.e., either a relatively strong hydrogen bond or no hydrogen bond, rather than a continuous distribution of all hydrogen-bond strengths. This bimodal behavior is dictated by the conformational constraints of the peptide backbone.

In the folded ensemble, the lower-frequency (hydrogen-bonded) peak is the stronger one for most sites, as expected (see Figure 3). Upon irradiation with 375 nm light, the peptide starts to unfold and clearly for L4 and L11 the intensity ratio of the two peaks reverses: more unbound C=O groups appear at positions 4 and 11. Surprisingly, L7 does exactly the opposite: the highest intensity is for the unbonded C=O group in the folded state. Upon unfolding, part of the intensity is transferred to the hydrogen-bonded peak. Nevertheless, this *per se* unexpected behavior of L7 is consistent with our previous kinetic studies of the folding process.<sup>24</sup> From the varying intensities of the hydrogen-bonded peaks, we conclude that the helical content is not uniform along the sequence. This conclusion is in line with work done by Huang et al.<sup>22</sup> and with our previous paper where we conclude that each site has its own folding kinetics.<sup>24</sup>

2D-IR spectroscopy efficiently suppresses the background contributions from numerous weaker bands, allowing two distinct peaks for hydrogen-bonded and non-hydrogen-bonded  $^{13}\text{C}^{18}\text{O}$  labels to be observed much more clearly in the 2D-IR spectra (Figure 3) than in the 1D spectra (Figure 2). This allows the quantification of the amount of hydrogen bonding of the various sites in both the folded and unfolded state. In the top panel of Figure 7, the diagonal cuts through the 2D-IR spectra from Figure 3 are depicted. The two peaks and the changes upon unfolding are clearly visible. The amount of hydrogen

bonding can be expressed as the ratio of the height of the hydrogen bonding peak at  $1570\text{ cm}^{-1}$  and the sum of the peak heights at  $1570$  and  $1590\text{ cm}^{-1}$ , which is shown in the bottom panel of Figure 7. All sites apart from site 7 show a decrease in the amount of hydrogen bonding upon unfolding, with the most pronounced change occurring for site 4. The appearance of two peaks for almost all sites even in the folded state indicates that it is actually not fully folded. According to CD spectroscopy, the folded state is  $\sim 70\%$  helical, in approximate agreement with the  $\sim 60\%$  hydrogen-bonded peptide units, when averaging over sites L4, L7, L9, and L11. Comparison of these numbers indicates that nonhelical peptide units actually are not hydrogen-bonded to any other partner, not even to surrounding water molecules. Hence, the amide groups we investigated here must sit in a relatively hydrophobic environment. Indeed, a small peptide in the nonprotic solvent acetonitrile showed the same high frequency (non-hydrogen-bonded) peak in an open conformation.<sup>7</sup> Presumably, the azobenzene switch shields the central part of the peptide from the solvent and is responsible for building an apolar core. Indeed, 2D-IR spectra of another helical peptide in water, without the azobenzene switch, were solely explained on the basis of various isotope substitutions.<sup>14,19</sup> However, the present study suggests that additional band splittings due to hydrogen bonding might play a role as well.

From CD, it is known that the helicity changes from 70 to 20% upon unfolding the peptide.<sup>24</sup> Interestingly, the fraction of hydrogen bonding changes much less (from  $\sim 60$  to  $\sim 45\%$ , averaged over sites L4, L7, L9, and L11). Apparently, the C=O group in the unfolded state finds other hydrogen bond partners, such as other backbone groups or lysine side chains. Although we cannot rigorously exclude that hydrogen bonding to water molecules plays a larger role in the unfolded state, this observation provides strong experimental evidence that one should think of the unfolded state more as misfolded, with many non-native contacts, i.e., backbone hydrogen bonds other than the  $\alpha$ -helical  $i \rightarrow i + 4$  hydrogen bonds and hydrogen bonds to the lysine residues. This conclusion is in full agreement with recent MD simulations.<sup>24,52</sup>

## Conclusion

2D-IR measurements on single  $^{13}\text{C}^{18}\text{O}$  isotope labels placed at different positions on a 16 residue helical photoswitchable peptide reveal clearly two amide I peaks at  $1570$  and  $1590\text{ cm}^{-1}$ . Modulating the folded state of the peptide with the photoswitch allows one to interpret these features as being due to hydrogen-bonded and non-hydrogen-bonded C=O groups of the peptide units. The similarity of the 2D-IR spectra of the single and double isotope labeled photoswitchable peptide samples illustrates that one has to be very careful when interpreting 2D-IR spectra. The spectra of the double labeled samples give the impression that both the  $^{13}\text{C}^{18}\text{O}$  and  $^{13}\text{C}^{16}\text{O}$  vibrations are visible, whereas the results from the single isotope labeled peptides unequivocally say that the two peaks have to be assigned to hydrogen-bonded versus non-hydrogen-bonded peptide units for most of the sites in the sequence. Clearly, 2D-IR spectra can be easily misinterpreted.

Cross-peaks in a 2D-IR spectrum are often used to give information about the structure of the molecule, because they indicate if two vibrations are in close vicinity.<sup>3-8</sup> Given the intrinsic high time resolution of 2D-IR spectroscopy, structural information can also be obtained during ultrafast conformational transitions. In other words, the appearance or disappearance of a cross-peak during a conformational transition could indicate that two molecular groups turn to each other or away from each

other, respectively, as recently illustrated for the opening of a  $\beta$ -turn.<sup>53</sup> Along this line, one might expect to follow folding or unfolding of an  $\alpha$ -helix by the change in cross-peak between the C=O group of amino acid *i* and the one of amino acid *i* + 3. As a protein or peptide has many C=O oscillators with all roughly the same vibrational frequency, double isotope labeling, e.g., <sup>13</sup>C<sup>18</sup>O and <sup>13</sup>C<sup>16</sup>O has to be used to get site specific information. Unfortunately, as shown in this paper, the <sup>13</sup>C<sup>16</sup>O band does in general not show up in the 2D-IR spectrum as an isolated vibration, so that a specific cross-peak between two C=O groups to follow the (un)folding is also not present in the spectrum. Recently, Meakawa et al.<sup>54</sup> have proposed an alternative approach. They used <sup>13</sup>C<sup>18</sup>O labeling in combination with <sup>15</sup>N labeling, and observed a cross-peak between the amide I mode of the amino acid with the <sup>13</sup>C<sup>18</sup>O label and the amide II mode of the amino acid with the <sup>15</sup>N label in a  $3_{10}$ -helix. This method of isotope labeling might open up the way to follow how two molecular groups in a helix turn to each other or away from each other in the folding process, which is one of the big goals in understanding protein folding.

As shown here, the diagonal peaks in a 2D-IR spectrum of an isotope labeled peptide give a great deal of information. The appearance of both the hydrogen-bonded and the non-hydrogen-bonded states provides an opportunity to unravel with unprecedented detail local hydrogen bond equilibria, at least in a hydrophobic environment, such as inside a protein. The two peaks are much clearer in the 2D-IR spectra than they are in the linear absorption spectra (compare Figure 2 with the cuts along the diagonal of the 2D-IR spectra in Figure 6). Upon unfolding or folding, the ratio of the two peaks clearly changes. This opens a way to study in great detail the local folding characteristics of the helix. We find that the helix is structurally heterogeneous even in the folded state. Furthermore, the averaged amount of hydrogen bonding in the folded state roughly parallels the helicity measured by CD spectroscopy, whereas both quantities differ significantly in the unfolded state. Hence, the unfolded state must form non-native contacts to either the peptide backbone or lysine side chains, and one should think of it more as misfolded rather than unfolded. In the future, we expect that transient 2D-IR experiments<sup>53</sup> will allow one to observe these hydrogen bond switching events during the folding process in greater detail.

**Acknowledgment.** This work is a result of a long-standing collaboration with Andrew Woolley (University of Toronto), whose constant input is highly appreciated. The work has been supported by the Swiss National Science Foundation (grant 200020-107492) and by the “Nederlandse organisatie voor Wetenschappelijk Onderzoek (NWO)” through a postdoc fellowship to E.H.G.B.

## References and Notes

- (1) Shim, S.-H.; Gupta, R.; Ling, Y. L.; Strasfeld, D. B.; Raleigh, D. P.; Zanni, M. T. *Proc. Natl. Acad. Sci. U.S.A.* **2009**, *106*, 6614.
- (2) Tokmakoff, A. *J. Phys. Chem. A* **2000**, *104*, 4247.
- (3) Woutersen, S.; Hamm, P. *J. Phys. Chem. B* **2000**, *104*, 11316.
- (4) Zanni, M. T.; Ge, N. H.; Kim, Y. S.; Hochstrasser, R. M. *Proc. Natl. Acad. Sci. U.S.A.* **2001**, *98*, 11265.
- (5) Demirdöven, N.; Cheatum, C. M.; Chung, H. S.; Khalil, M.; Knoester, J.; Tokmakoff, A. *J. Am. Chem. Soc.* **2004**, *126*, 7981.
- (6) Larsen, O. F. A.; Bodis, P.; Buma, W. J.; Hannam, J. S.; Leigh, D. A.; Woutersen, S. *Proc. Natl. Acad. Sci. U.S.A.* **2005**, *102*, 13378.
- (7) Cervetto, V.; Pfister, R.; Kolano, C.; Bregy, H.; Heimgartner, H.; Helbing, J. *Chem.—Eur. J.* **2007**, *13*, 9004.
- (8) Jansen, T. I. C.; Knoester, J. *Biophys. J.* **2008**, *94*, 1818.
- (9) Woutersen, S.; Mu, Y.; Stock, G.; Hamm, P. *Chem. Phys.* **2001**, *266*, 137.
- (10) Finkelstein, I. J.; Zheng, J.; Ishikawa, H.; Kim, S.; Kwak, K.; Fayer, M. D. *Phys. Chem. Chem. Phys.* **2007**, *9*, 1533.
- (11) Anna, J. M.; Ross, M. R.; Kubarych, K. J. *J. Phys. Chem. A* **2009**, *113*, 6544.
- (12) Hamm, P.; Lim, M.; DeGrado, W. F.; Hochstrasser, R. M. *J. Chem. Phys.* **2000**, *112*, 1907.
- (13) Zanni, M. T.; Gnanakaran, S.; Stenger, J.; Hochstrasser, R. M. *J. Phys. Chem. B* **2001**, *105*, 6520.
- (14) Fang, C.; Wang, J.; Kim, Y. S.; Charnley, A. K.; Barber-Armstrong, W.; Smith, A. B.; Decatur, S. M.; Hochstrasser, R. M. *J. Phys. Chem. B* **2004**, *108*, 10415.
- (15) Shim, S.-H.; Strasfeld, D. B.; Ling, Y. L.; Zanni, M. T. *Proc. Natl. Acad. Sci. U.S.A.* **2007**, *104*, 14197.
- (16) Fournier, F.; Gardner, E. M.; Kedra, D. A.; Donaldson, P. M.; Guo, R.; Butcher, S. A.; Gould, I. R.; Willison, K. R.; Klug, D. R. *Proc. Natl. Acad. Sci. U.S.A.* **2008**, *105*, 15352.
- (17) Fang, C.; Senes, A.; Cristian, L.; DeGrado, W. F.; Hochstrasser, R. M. *Proc. Natl. Acad. Sci. U.S.A.* **2006**, *103*, 16740.
- (18) Mukherjee, P.; Kass, I.; Arkin, I. T.; Zanni, M. T. *Proc. Natl. Acad. Sci. U.S.A.* **2006**, *103*, 3528.
- (19) Fang, C.; Hochstrasser, R. M. *J. Phys. Chem. B* **2005**, *109*, 18652.
- (20) Torii, H.; Tatsumi, T.; Tasumi, M. *Mikrochim. Acta* **1997**, *14*, 531.
- (21) Kwac, K.; Lee, H.; Cho, M. *J. Chem. Phys.* **2004**, *120*, 1477.
- (22) Huang, C.-Y.; Getahun, Z.; Zhu, Y.; Klemke, J. W.; DeGrado, W. F.; Gai, F. *Proc. Natl. Acad. Sci. U.S.A.* **2002**, *99*, 2788.
- (23) Brewer, S. H.; Song, B.; Raleigh, D. P.; Dyer, R. B. *Biochemistry* **2007**, *46*, 3279.
- (24) Ihalainen, J. A.; Paoli, B.; Muff, S.; Backus, E. H. G.; Bredenbeck, J.; Woolley, G. A.; Caffisch, A.; Hamm, P. *Proc. Natl. Acad. Sci. U.S.A.* **2008**, *105*, 9588.
- (25) Williams, S.; Causgrove, T. P.; Gilmanshin, R.; Fang, K. S.; Callender, R. H.; Woodruff, W. H.; Dyer, R. B. *Biochemistry* **1996**, *35*, 691.
- (26) Scholtz, J. M.; Marqusee, S.; Baldwin, R. L.; York, E. J.; Stewart, J. M.; Santoro, M.; Bolen, D. W. *Proc. Natl. Acad. Sci. U.S.A.* **1991**, *88*, 2854.
- (27) Muñoz, V.; Serrano, L. *J. Mol. Biol.* **1995**, *245*, 297.
- (28) Thompson, P. A.; Eaton, W. A.; Hofrichter, J. *Biochemistry* **1997**, *36*, 9200.
- (29) Werner, J. H.; Dyer, R. B.; Fesinmeyer, R. M.; Andersen, N. H. *J. Phys. Chem. B* **2002**, *106*, 487.
- (30) Kumita, J. R.; Smart, O. S.; Woolley, G. A. *Proc. Natl. Acad. Sci. U.S.A.* **2000**, *97*, 3803.
- (31) Bredenbeck, J.; Helbing, J.; Kumita, J. R.; Woolley, G. A.; Hamm, P. *Proc. Natl. Acad. Sci. U.S.A.* **2005**, *102*, 2379.
- (32) Ihalainen, J. A.; Bredenbeck, J.; Pfister, R.; Helbing, J.; Chi, L.; Stokkum, I. H. M. v.; Woolley, G. A.; Hamm, P. *Proc. Natl. Acad. Sci. U.S.A.* **2007**, *104*, 5383.
- (33) Aemissegger, A.; Kräutler, V.; Gunsteren, W. F. v.; Hilvert, D. *J. Am. Chem. Soc.* **2005**, *127*, 2929.
- (34) Dong, S.-L.; Löweneck, M.; Schrader, T. E.; Schreiber, W. J.; Zinth, W.; Moroder, L.; Renner, C. *Chem.—Eur. J.* **2006**, *12*, 1114.
- (35) Wachtveitl, J.; Sporlein, S.; Satzger, H.; Fonrobert, B.; Renner, C.; Behrendt, R.; Oesterhelt, D.; Moroder, L.; Zinth, W. *Biophys. J.* **2004**, *86*, 2350.
- (36) Arkin, I. T. *Curr. Opin. Chem. Biol.* **2006**, *10*, 394.
- (37) Decatur, S. M.; Antonic, J. *J. Am. Chem. Soc.* **1999**, *121*, 11914.
- (38) Barber-Armstrong, W.; Donaldson, T.; Wijesooriya, H.; Silva, R. A. G. D.; Decatur, S. M. *J. Am. Chem. Soc.* **2004**, *126*, 2339.
- (39) Koziński, M.; Garrett-Roe, S.; Hamm, P. *Chem. Phys.* **2007**, *341*, 5.
- (40) Volkov, V.; Schanz, R.; Hamm, P. *Opt. Lett.* **2005**, *30*, 2010.
- (41) Garrett-Roe, S.; Hamm, P. *J. Chem. Phys.* **2009**, *130*, 164510.
- (42) Fulmer, E. C.; Mukherjee, P.; Krummel, A. T.; Zanni, M. T. *J. Chem. Phys.* **2004**, *120*, 8067.
- (43) Bloem, R.; Garrett-Roe, S.; Hamm, P. In preparation, 2010.
- (44) Faeder, S. M. G.; Jonas, D. M. *J. Phys. Chem. A* **1999**, *103*, 10489.
- (45) Murphy, R. C.; Clay, K. L. *Methods Enzymol.* **1990**, *193*, 338.
- (46) Pfister, R.; Ihalainen, J.; Hamm, P.; Kolano, C. *Org. Biomol. Chem.* **2008**, *6*, 3508.
- (47) Hamm, P.; Lim, M.; Hochstrasser, R. M. *J. Phys. Chem. B* **1998**, *102*, 6123.
- (48) Hamm, P.; Woutersen, S. *Bull. Chem. Soc. Jpn.* **2002**, *75*, 985.
- (49) Bredenbeck, J.; Hamm, P. *J. Chem. Phys.* **2003**, *119*, 1569.
- (50) Krivov, S. V.; Karplus, M. *Proc. Natl. Acad. Sci. U.S.A.* **2004**, *101*, 14766.
- (51) Cervetto, V.; Hamm, P.; Helbing, J. *J. Phys. Chem. B* **2008**, *112*, 8398.
- (52) Paoli, B.; Seeber, M.; Backus, E. H. G.; Ihalainen, J. A.; Hamm, P.; Caffisch, A. *J. Phys. Chem. B* **2009**, *113*, 4435.
- (53) Kolano, C.; Helbing, J.; Koziński, M.; Sander, W.; Hamm, P. *Nature* **2006**, *444*, 469.
- (54) Maekawa, H.; Poli, M. D.; Toniolo, C.; Ge, N.-H. *J. Am. Chem. Soc.* **2009**, *131*, 2042.